

Infiltration of Nanoparticles into Porous Binder Jet Printed Parts

¹Amelia Elliott, ²Sarah AlSalihi, ³Abbey L. Merriman and ⁴Mufeed M. Basti

^{1,3}Manufacturing Demonstration Facility, Oak Ridge National Laboratory, Oak Ridge, Tennessee, USA

²Department of Chemical Engineering, North Carolina A&T University, Greensboro, North Carolina, USA

⁴Department of Chemistry, North Carolina A&T University, Greensboro, North Carolina, USA

Article history

Received: 02-26-2016

Revised: 01-03-2016

Accepted: 01-03-2016

Corresponding Author:

Mufeed M. Basti

Department of Chemistry, North Carolina A&T University, Greensboro, North Carolina, USA

Email: basti@ncat.edu

Abstract: The densification of parts that are produced by binder jetting Additive Manufacturing (AM; a.k.a. “3D Printing”) is an essential step in making them mechanically useful. Increasing the packing factor of the powder bed by incorporating nanoparticles into the binder has potential to alleviate the amount of shrinkage needed for full densification of binder jet parts. In this study we present preliminary data on the use of 316L Stainless Steel Nanoparticles (SSN) to densify 316L stainless steel binder jet parts. Aqueous solutions of Diethylene Glycol (DEG) or Ethylene Glycol (EG) were prepared at different DEG/water and EG/water molar ratios; pH of the solutions was adjusted by the use of 0.10 M sodium hydroxide. Nanoparticles were suspended in a resulted solution at a volume percentage of SSN/solution at 0.5%. The suspension was then sonicated for thirty minutes. One milliliter of the suspension was added stepwise to a sintered, printed disk with the dimensions: (d = 10 mm, h = 3 mm) in the presence of a small magnet. The 3D part was then sintered again. The increase in the mass of the 3D part was used as indication of the amount of nanoparticles that diffused in the 3D part. This mass percent increase was studied as a function of pH of the suspension and as function DEG/water molar ratio. Unlike EG, data show that change in pH affects the mass percent when the suspension was made with DEG. Optical analysis of the discs’ cross sections revealed trends metallic densities similar to trends in the data for mass increase with changing pH and water molar ratio.

Keywords: Nanoparticles, Additive Manufacturing, 3D Printing, Metal Powder

Introduction

Additive Manufacturing (AM; a.k.a. “3D Printing”) has now many industrial applications such as in aerospace, in medical and in engineering and scientific fields (Leukers *et al.*, 2005; Hockaday *et al.*, 2012). AM of metals typically starts with a with metal powder and shapes the powder feedstock in a number of ways such as direct metal laser sintering (Khaing *et al.*, 2001), selective laser sintering (Silva *et al.*, 2008) and binder jetting (Allen and Sachs, 2000). In the latter method, layers of metal powder are spread and binder is selectively deposited via inkjet until the 3D part is built according to the design. After deposition, the entire print bed is heated to 200°C to cure the binder and solidify the printed shape. The resulting “green”

printed shape, also called the skeleton, can be removed from the powder bed and set up for infiltration and sintering.

Because of the low cost of the technology and high throughputs, binder jetting has the potential to surpass many other metal AM processes in utility for industrial applications. However, a major challenge for binder jet AM is the porosity of the printed part and the subsequent inability to reach full density with a single alloy without significant shrinkage and warpage. For typical powders, the density of the green part is almost 60% by volume while the other 40% is open porosity. The fundamental cause for the low density of the green parts is the packing factor of the powder feedstock. Increasing the packing factor of the feedstock powder by filling the void space with

smaller particles means that objects with densities up to 86.8% can be printed (Rahaman, 2003).

Potentially, utilizing nanoparticles will not only fill the void space but also act as a sintering aid (Koparde and Cummings, 2008). The incorporation of metal nanoparticles in AM has a great interest to researchers since nanoparticles can bring the multi-functionality aspect, such as thermal and electric conductivity, to AM (Crane *et al.*, 2005). It was also shown that adding nanomaterials to AM can improve mechanical properties, lower sintering temperatures and improve dimensional accuracy (Bai *et al.*, 2007; Cutler *et al.*, 1957). One of the first reports on using metal nanoparticles in AM was by Crane *et al.* (2005) where iron nanoparticles (diameter 7-10 nm) were used to improve the quality of 410 Stainless Steel (SS) 3D parts where the particle size of the SS was 63-90 μm . The application of nanoparticles was repeated to increase the quantity of the deposited nanoparticles and the work showed that applying the nanoparticles reduced both creep and deflection of the AM.

The ideal scenario for nanoparticle delivery is suspending the nanoparticles within the binder itself and as the binder is deposited via inkjet into the powder bed, the nanoparticles are deposited as well. As a preliminary step to determine the effect of the nanoparticles, in this study we investigate the infiltration of 316L stainless steel 3D parts by 316 L nanoparticles. It is hypothesized that the dispersion of the nanoparticles within the liquid carrier affects the amount of material delivered to the print. Stainless steel nanoparticles were added to binder jet printed stainless steel skeletons via suspending the particles in water mixed with two different liquid polymer carriers and depositing drop-wise. The pH of the liquid polymer as well as the polarity determines the stability and dispersion of the suspension. The samples were sintered and measured for increases in mass and density to determine the effectiveness of the infiltration technique.

Experimental Program

Methodology

Ethylene Glycol (EG) or Polyethylene Glycol (PEG) are used as binder in binder jetting AM (Hockaday *et al.*, 2012). PEG is a homo copolymer that comprises two or more identical subunits (glycols) that are linked by covalent bonds (Lee *et al.*, 2003) (ether bond: R-O-R'). PEG is also frequently used in binder jetting that uses ceramics as the skeleton material (Ekka, 2012). Halidi and

Abdullah (2012) have studied the effects of polyethylene glycol on Hydroxyapatite Powder (HAP)-binder system for AM applications. Table 1 shows the physical properties of ethylene glycol and different polyethylene glycol polymers. It includes: Monoethylene Glycol (MEG); Diethylene Glycol (DEG); Triethylene Glycol (TEG); and Tetraethylene Glycol (TETRA EG). The data was obtained from The Dow Chemical Company website.

L-grade 316L Stainless Steel Nanoparticles (SSN) (60-80 nm) were purchased from SkySpring Nanomaterials, Houston, TX, USA. The composition of SSN as supplied by the manufacturer is Fe 62.045-72%, Cr 16-18%, Ni 10-14%, Mo 2-3%, Mn 2%, N 0.1%, S 0.03%, C 0.03%, Si 0.75% and P 0.045%. Sodium hydroxide was purchased from Fisher Scientific, New Jersey, USA and used with no further purification. Ethylene Glycol (EG) and Diethylene glycol (DE) were purchased from ExOne Company, North Huntingdon, PA, USA. The solutions of deionized water/Ethylene Glycol (EG) and deionized water/Diethylene Glycol (DEG) were made at EG/water and DEG/water molar ratios between 1/1 and 1/12. The pH was altered between the range of 8 and 14 by the drop-wise addition 0.10 M NaOH solution and the pH was monitored using a Sper Scientific 860031 Benchtop pH meter. The concentration of SSN in the EG/water and DEG/water solutions was maintained at 0.175 g SSN and 4.22 mL of EG/H₂O or DEG/H₂O solution. The SSN suspension was then placed in a 10 mL conical tube and the tube was immersed in a bath sonicator for 30 min at room temperature to improve the dispersion of SSN.

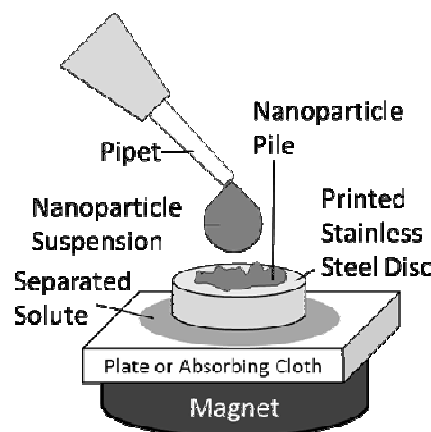


Fig. 1. Experimental setup and subsequent separation of the suspension

Table 1. Physical properties of ethylene glycol and different polyethylene glycol polymers

Physical Properties	MEG	DEG	TEG	TETRA EG
Formula	C ₂ H ₆ O ₂	C ₄ H ₁₀ O ₄	C ₆ H ₁₄ O ₄	C ₈ H ₁₈ O ₅
Molecular weight, g/mol	62	106.12	150	194.2
Boiling point at 760 mm Hg, °C	197	245	288	329
Density, (g/cc) at 20°C	1.115	1.118	1.125	1.124

Stainless steel discs 10 mm in diameter and 3 mm tall and a mass close to 1 g were printed on ExOne's 3D printer using 316L stainless steel metal powder (size of the particles is 30-50 microns) and DEG as binder. The 3D parts were sintered at 1,100°C in 96% Ar/4% H₂ gas atmosphere for 30 min. The discs were placed on a cloth or plate and 100 µL of the SSN suspension were pipetted on top of it using 100 µL micropipette. Total volume of the added suspension was 1 mL. A small magnet was placed underneath the plastic plate or cloth to attract the nanoparticles to the surface of the 3D print.

When soaked from the top with the nanoparticle suspension, the porous disc prints acted as a filter separating the nanoparticles from suspension. The clear fluid from the suspension was drawn out with the absorbing cloth and the nanoparticles became piled atop the printed disc. Figure 1 is a depiction of the deposition setup and the resulting separation. The 3D print was then sintered again at 1,100°C in 96% Ar/4% H₂ gas atmosphere for thirty minutes.

Results

The effectiveness of the polymer solute to deliver the nanoparticles was assessed by the measuring the increase in the mass of the 3D parts after the application of nanoparticles and subsequent sintering. This increase in mass is shown as mass percent increase. Figure 2 shows the effect of pH of DEG/H₂O and EG/H₂O solutions on the mass percent increase of the 3D part (Molar ratio of DEG/H₂O and EG/H₂O is 1/4). The figure shows that change in pH has no effect on mass percent when nanoparticles were suspended in EG/H₂O solution, while the change in pH significantly affects the mass percent when

nanoparticles were suspended in DEG/H₂O solution. The presence of the oxygen atom in the middle of DEG molecule makes it more polar than EG (the general chemical formula of DEG is R-O-R where R is OH-CH₂-CH₂ and the formula of EG is OH-CH₂-CH₂-OH). This higher polarity can be used to explain the higher effect of pH on DEG than on EG.

Select samples reported in Fig. 2 were polished and imaged for density using standard metallography techniques and image analysis software. The software turns the optical microscope image into a black and white schematic (black being the pores and white being the metallic portions) and analyzes these regions for density. The samples were measured in four regions along the thickness of the discs: Top, top middle, bottom middle and bottom. Examples of the black and white images from the cross-sectioned disc samples can be seen in Fig. 3. Similar analyses were carried out on other samples where the suspension was made with DEG or EG at different pH values. As Fig. 4 shows, the density of the treated stainless steel discs increases at a pH of 11 for DEG, similar to what is seen in Fig. 2. The density analysis shows also an increase in density for the EG sample as well at a pH of 11. The slightly higher density that can be seen in Fig. 3A than in Fig. 3B correlates to the data in Fig. 4.

Figure 2 indicates that DEG/H₂O suspension at pH 11 yields a high mass percent increase in the printed discs. The effect of DEG/H₂O molar ratio on the mass percent increase was then carried out at pH 11. Figure 5 shows that DEG/water molar ratio of 1:4 gives the best mass percent value. Select samples reported in Fig. 5 were polished and imaged for density as was reported in Fig. 4. The results are shown in Fig. 6.

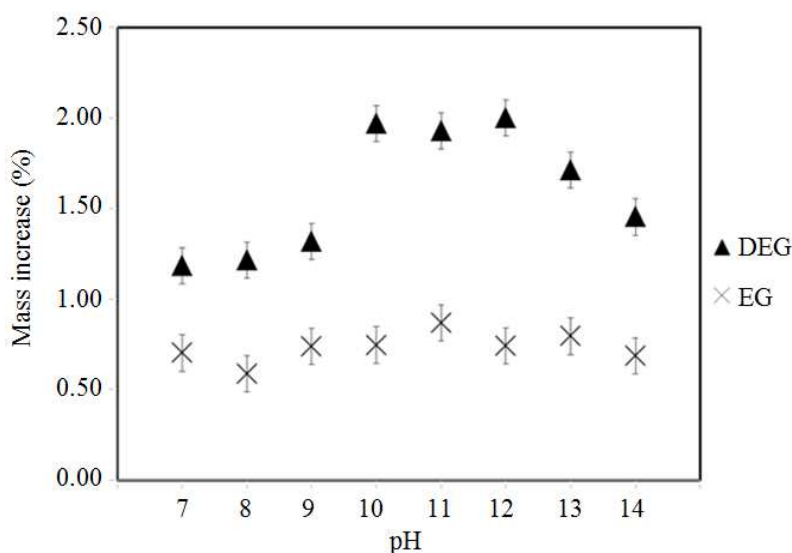


Fig. 2. Effect of pH on the mass increase percentage

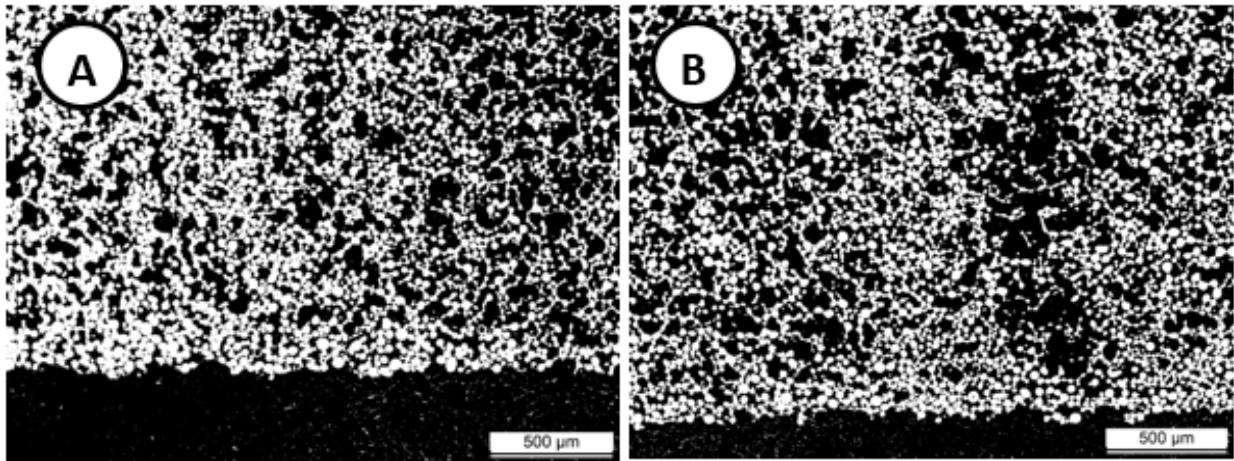


Fig. 3. Cross section of sintered disc treated with nanoparticle solution with a pH of 11 and with (A) EG/water and (B) DEG/water ratios of 1:4

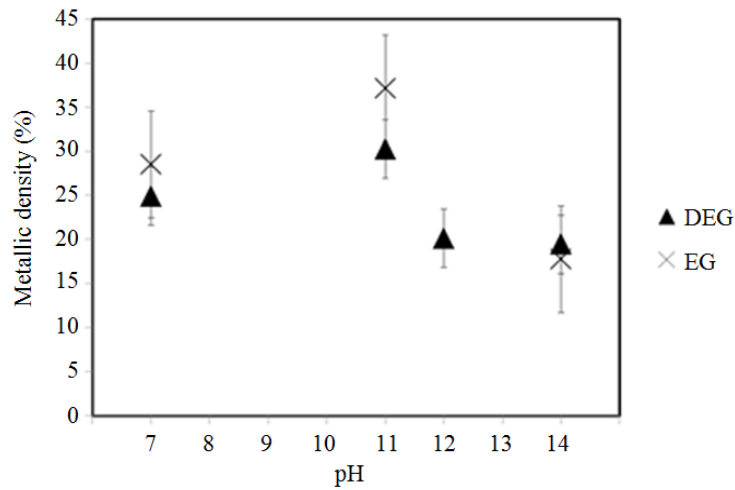


Fig. 4. Density of the sintered samples with increasing pH of the solutions with DEG and EG (measured optically)

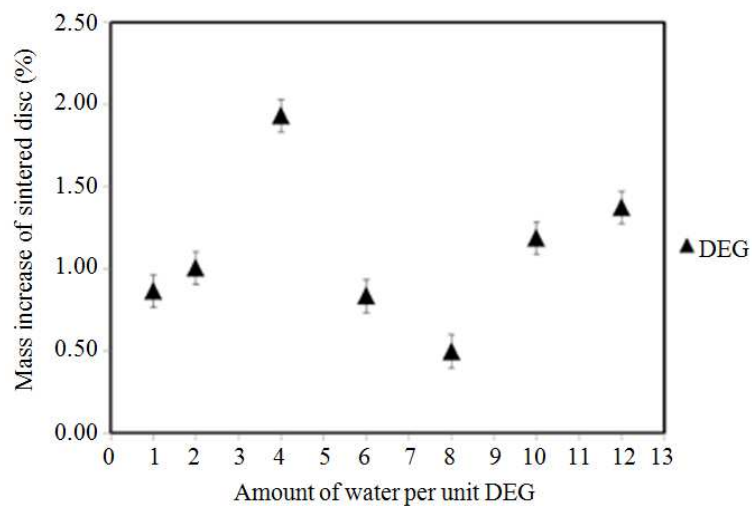


Fig. 5. Effect of DEG: H₂O molar ratio on the mass increase percentage at pH 11

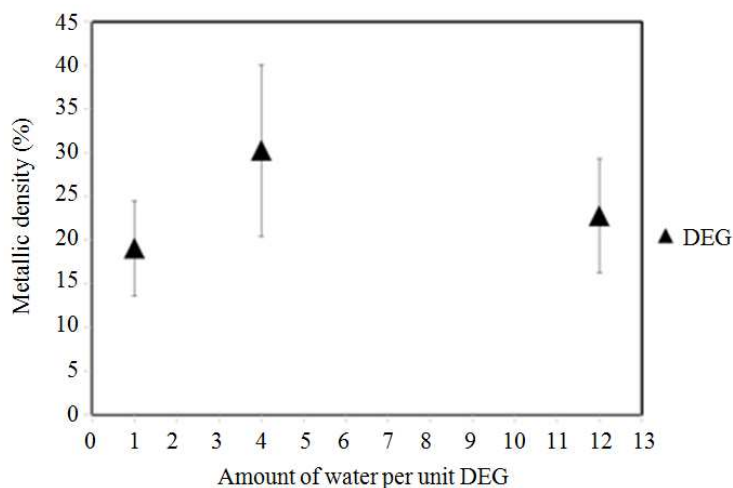


Fig. 6. Density of the sintered samples at different DEG: H₂O molar ratios at pH 11 (measured optically)

Discussion

The significant changes in the mass per cent as the DEG/H₂O molar ratio changes (Fig. 5) can be explained by the change in the pattern of hydrogen bonding between H₂O and DEG molecules. Specifically, DEG molecule has three oxygen atoms that participate in hydrogen bonding with water. When an oxygen atom of DEG participates in hydrogen bonding, the partial negative charge on it is reduced which affects how DEG molecules repel each other. Such change in repulsion forces affects how the nanoparticles are dispersed in the suspension. It is hypothesized that an increase in repulsion forces between the DEG molecules will increase the dispersion of the nanoparticles in solution. Such increase in dispersion will enhance the degree of nanoparticles incorporation in the 3D part and in turn increase the 3D part mass. Figure 5 suggests that when DEG/H₂O molar ratio is 1:4 the repulsion forces between DEG molecules are at maximum level. The results in Fig. 5 are corroborated by optical density analysis reported in Fig. 6.

Conclusion

A set of experiments was conducted to evaluate the effect of pH and molar ratio with water of DEG and EG polymers on conveying nanoparticles through sintered, additively manufactured, stainless steel discs. Through mass measurements, the solutions with DEG added the most weight at a pH of 11 while both DEG and EG saw an increase in density at the same pH as measured by optical density analysis. The higher polarity of the DEG and subsequent better dispersion and infiltration of the nanoparticles could be the cause of the increase in weight for certain pH

levels. The optical density results, however, point to gains in metallic mass with both DEG and EG at a pH of 11. The final analysis shows that a ratio of Water: DEG of 1:4 produces the highest weight gains as well as metallic density. Further analysis is needed to determine the effects of surface tension and viscosity of each of the mixtures on penetration of the nanoparticles into the sintered discs. This work is a step toward incorporating nanoparticles within binder jet printing fluids to increase the density and sinterability of binder jet printed parts.

Acknowledgment

The authors would like to acknowledge the Minority Serving Institutions and Partnerships Program and the Department of Energy for supporting this work.

Funding Information

The work reported here was financially supported by the National Nuclear Security Administration (NNSA)-Minority Serving Institutions and Partnerships Program.

Author's Contributions

Amelia Elliott: Participated in all experimental testing, data-analysis and contributed to the writing of the manuscript.

Sarah AlSalih: Participated in experimental plan and testing, data-analysis and contributed to the writing of the manuscript.

Abbey L. Merriman: Participated in experimental plan, data-analysis and contributed to the writing of the manuscript.

Mufeed M. Basti: Participated in experimental plan, data-analysis and contributed to the writing of the manuscript.

Ethics

All rights reserved. No part of this publication may be reproduced or transmitted in any form or by any means, electronic or mechanical, including photocopy, or any information storage and retrieval system, without permission in writing from the publisher or authors.

Reference

- Allen, S.M. and E.M. Sachs, 2000. Three-dimensional printing of metal parts for tooling and other applications. *Met. Mater.*, 6: 589-594.
DOI: 10.1007/BF03028104
- Bai, J.G., K.D. Creehan and H.A. Kuhn, 2007. Inkjet printable nanosilver suspensions for enhanced sintering quality in rapid manufacturing. *Nanotechnology*, 18: 185701-185701.
DOI: 10.1088/0957-4484/18/18/185701
- Crane, N.B., J. Wilkes, E. Sachs and S.M. Allen, 2005. Improving accuracy of powder sintering-based SFF processes by metal deposition from nanoparticle dispersion.
- Cutler, I.B., C. Bradshaw, C.J. Christensen and E.P. Hyatt, 1954. Sintering of alumina at temperatures of 1400°C and below. *J. Am. Ceram. Soc.*, 40: 134-139.
DOI: 10.1111/j.1151-2916.1957.tb12589.x
- Ekka, P., 2012. Effect of binders and plasticisers on alumina processing. B.Tech Thesis, National Institute of Technology Rourkela.
- Halidi, S.N.A.M. and J. Abdullah, 2012. Moisture effects on the ABS used for fused deposition modeling rapid prototyping machine. Proceedings of the IEEE Symposium on Humanities, Science and Engineering Research, Jun. 24-27, IEEE Xplore Press, Kuala Lumpur, pp: 839-843.
DOI: 10.1109/SHUSER.2012.6268999
- Hockaday, L.A., K.H. Kang, N.W. Colangelo, P.Y.C. Cheung and B. Duan *et al.*, 2012. Rapid 3D printing of anatomically accurate and mechanically heterogeneous aortic valve hydrogel scaffolds. *Biofabrication*, 4: 035005-035005.
DOI: 10.1088/1758-5082/4/3/035005
- Khaing, M.W., J.Y.H. Fuh and L. Lu, 2001. Direct metal laser sintering for rapid tooling: Processing and characterisation of EOS parts. *J. Mater. Process. Technol.*, 113: 269-272.
DOI: 10.1016/S0924-0136(01)00584-2
- Koparde, V.N. and P.T. Cummings, 2008. Sintering of titanium dioxide nanoparticles: A comparison between molecular dynamics and phenomenological modeling. *J. Nanoparticle Res.*, 10: 1169-1182.
DOI: 10.1007/s11051-007-9342-3
- Lee, E.S., H.J. Shin, K. Na and Y.H. Bae, 2003. Poly(L-histidine)-PEG block copolymer micelles and pH-induced destabilization. *J. Control. Release*, 90: 363-374. DOI: 10.1016/S0168-3659(03)00205-0
- Leukers, B., H. Gülkan, S.H. Irsen, S. Milz and C. Tille *et al.*, 2005. Hydroxyapatite scaffolds for bone tissue engineering made by 3D printing. *J. Mater. Sci. Mater. Med.*, 16: 1121-1124.
DOI: 10.1007/s10856-005-4716-5
- Rahaman, M.N., 2003. *Ceramic Processing and Sintering*. 2nd Edn., CRC Press, Boca Raton, FL., ISBN-10: 0824709888, pp: 875.
- Silva, D.N., M. Gerhardt de Oliveira, E. Meurer, M.I. Meurer and J.V. Lopes da Silva *et al.*, 2008. Dimensional error in selective laser sintering and 3D-printing of models for craniomaxillary anatomy reconstruction. *J. Cranio-Maxillofacial Surg.*, 36: 443-449. DOI: 10.1016/j.jcms.2008.04.003